

Optical detection of the X-ray flash in the very fast nova V1674 Her: Optical contribution of the irradiated accretion disk

IZUMI HACHISU ¹ AND MARIKO KATO ²

¹*Department of Earth Science and Astronomy, College of Arts and Sciences, The University of Tokyo, 3-8-1 Komaba, Meguro-ku, Tokyo 153-8902, Japan*

²*Department of Astronomy, Keio University, Hiyoshi, Kouhoku-ku, Yokohama 223-8521, Japan*

ABSTRACT

V1674 Her is one of the fastest and brightest novae, characterized by dense optical photometry in the pre-maximum phase, a rise from $g = 17$ to 7 mag, in one-fourth of a day. We present a composite theoretical V light curve model of its early rising phase starting from a quiescent brightness of $g = 19.2$ mag. Our light curve model consists of a hot and bright white dwarf (WD) and irradiated accretion disk and companion star. We found that the earliest optical detection of ASAS-SN g band brightness of $g = 17.0$ at $t = 0.014$ day from the onset of thermonuclear runaway can be explained with the irradiated accretion disk and companion star in the X-ray flash phase of a $1.35 M_{\odot}$ WD. This is the first detection in optical of an X-ray flash phase of a nova. Optically thick winds emerge from the WD photosphere at $t = 0.04$ day, and optical flux is dominated by free-free emission from optically-thin ejecta just outside the WD photosphere. Our free-free emission model V light curve reasonably reproduces the dense g light curve of Evryscope that spans from $g = 14.8$ (at 0.078 day) to $g = 7.1$ (at 0.279 day), including a sudden change of slope in the g light curve from slow to rapid rise at $g = 14.3$ on day 0.1. There is no indication of shocking power during the rising phase from $g = 14.8$ to 7.1.

Keywords: novae, cataclysmic variables — stars: individual (V1674 Her) — stars: winds — X-rays: stars

1. INTRODUCTION

A nova is a thermonuclear runaway event on a mass accreting white dwarf (WD). After hydrogen ignites at the bottom of the WD envelope, the WD brightens up and its hydrogen-rich envelope expands largely to emit strong winds (e.g., M. Kato et al. 2022a, for a recent fully self-consistent nova outburst model). Many classical novae have ever been detected only after or close to their optical maxima. Therefore, their very early pre-maximum phases have not been studied in detail.

One of the rare exceptions is the X-ray flash detection in the classical nova YZ Ret (O. König et al. 2022). An X-ray flash is a soft X-ray bright event of a nova just after the thermonuclear runaway starts, typically a few days before optical maximum in very massive WDs like in YZ Ret (M. Kato et al. 2022b,c). From an

X-ray spectrum analysis of YZ Ret, O. König et al. (2022) found no major intrinsic absorption during the X-ray flash. Comparing the YZ Ret X-ray data with their model calculations, M. Kato et al. (2022b) concluded that, in such an early phase of a nova outburst, (1) no dense matter exists around the WD photosphere, (2) no indication of a shock wave, and (3) the hydrogen-rich envelope is almost hydrostatic. These conclusions are very consistent with their theoretical models in which massive optically thick winds emerge from the WD photosphere only after the X-ray flash phase ended.

Another rare exception is the very fast nova V1674 Her (Nova Herculis 2021) discovered on UT 2021 June 12.537 by Seiji Ueda (cf. CBET 4976). This object has been observed in multiwavelength, from radio, optical, UV, X-ray, to gamma-ray (e.g., J. J. Drake et al. 2021; C. E. Woodward et al. 2021; C.-C. Lin et al. 2022; J. Patterson et al. 2022; M. Orio et al. 2022; K. V. Sokolovsky et al. 2023; Y. Bhargava et al. 2024; G.

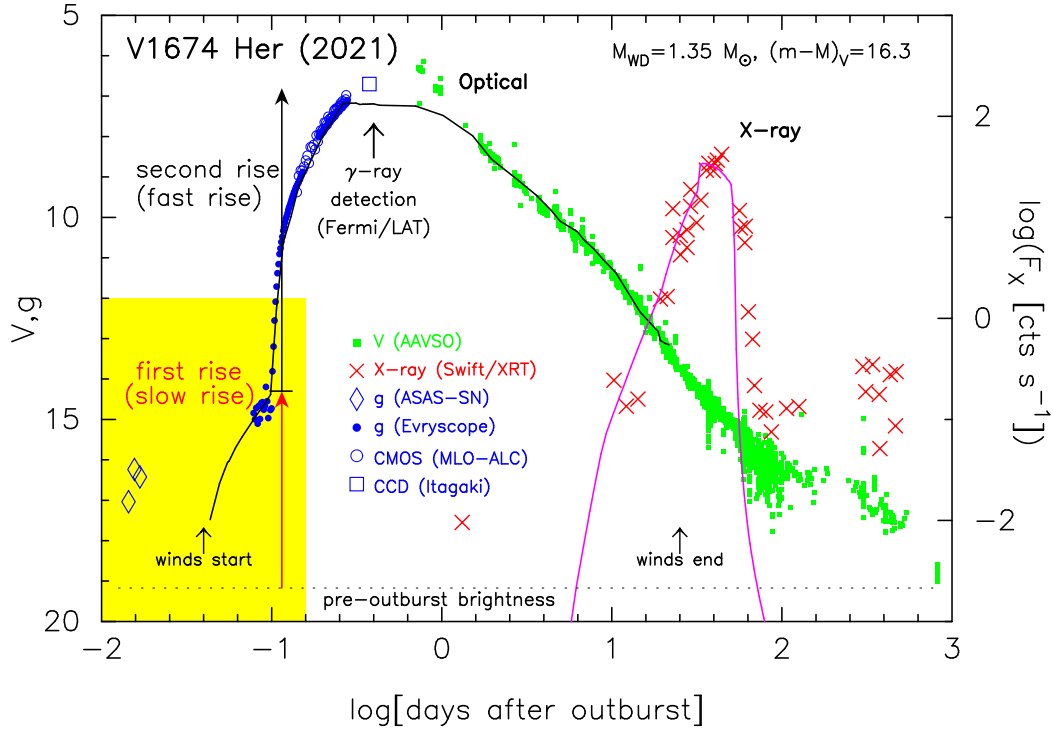


Figure 1. The optical V/g and X-ray (0.3–10.0 keV) light curves of V1674 Her. The V data are taken from the archive of the American Association of Variable Star Observers (AAVSO). The All-Sky Automated Survey for Supernovae (ASAS-SN) g , Evryscope g , and Itagaki’s unfiltered CCD data are from R. M. Quimby et al. (2024). The X-ray count rates are from the Swift website (P. A. Evans et al. 2009). The Mount Laguna Observatory All-Sky Camera (MLO-ASC) data are from K. V. Sokolovsky et al. (2023). We add a theoretical V and X-ray light curve based on M. Kato et al. (2025)’s fully self-consistent nova outburst model. We set our theoretical outburst day (stage B in Figure 2) to be HJD 2,459,377.68. The white dwarf (WD) model has the mass of $M_{\text{WD}} = 1.35 M_{\odot}$ with the mass-accretion rate of $\dot{M}_{\text{acc}} = 1 \times 10^{-11} M_{\odot} \text{ yr}^{-1}$. The model V light curve (black line) is calculated from free-free emission from nova winds whereas the model X-ray light curve (magenta line) is calculated from the blackbody emission from the photosphere (0.3–10.0 keV). The V band distance modulus $\mu_V \equiv (m - M)_V = 16.3$, the distance $d = 8.9$ kpc, and the extinction $E(B - V) = 0.5$ are taken from M. Kato et al. (2025). There is a sudden slope change (a break of the black line) in the rising phase, as demonstrated in the yellow-shadowed area. We divide the rising phase into two, before and after the break as shown by the red and black upward arrows. We also show the quiescent brightness of $g = 19.17$ (dotted line; R. M. Quimby et al. 2024) 1.7 days before the nova outburst ($t = -1.7$ day).

R. Habtie et al. 2024; R. M. Quimby et al. 2024). Early observations are summarized in J. J. Drake et al. (2021), K. V. Sokolovsky et al. (2023), Y. Bhargava et al. (2024), and R. M. Quimby et al. (2024).

A remarkable feature is dense optical photometric data in the rising phase, which is shown in Figure 1. The source of each data can be found in the caption. A plenty of optical data were obtained from $g = 17.0$ to $g = 7$, over 10 magnitudes rise only during one-fourth of a day (K. V. Sokolovsky et al. 2023; R. M. Quimby et al. 2024).

This plot also shows a theoretical free-free emission model V light curve (black line) and X-ray (0.3–10 keV) light curve in the supersoft X-ray source (SSS) phase (magenta line), the data of which are taken from M. Kato et al. (2025) for a $1.35 M_{\odot}$ WD with a mass accretion rate of $1 \times 10^{-11} M_{\odot} \text{ yr}^{-1}$. Their model V light curve reproduces overall properties of the observed

data, from the very fast rising phase of $V \sim 14$ mag until the end of the outburst. This is the first successful model that reproduces the rapid rise of a classical nova in the very early phase.

M. Kato et al. (2025) did not show the earliest rising phase from the quiescent brightness of $g = 19.17$ to $g \sim 14$ mag. The ASAS-SN g data (open blue diamonds) seems to be in a different stream from the Evryscope data (blue dots). The aim of this paper is to elucidate this very early phase of the outburst of V1674 Her with a binary model including irradiation effect by the hot and bright WD. Our V light curve model consists of the exploding WD (taken from M. Kato et al. (2025)’s $1.35 M_{\odot}$ WD model), disk and companion star both irradiated by the hot and bright WD.

This paper is organized as follows. First we explain the one cycle of the nova outburst in the H-R diagram based on the $1.35 M_{\odot}$ WD model (M. Kato et al. 2025)

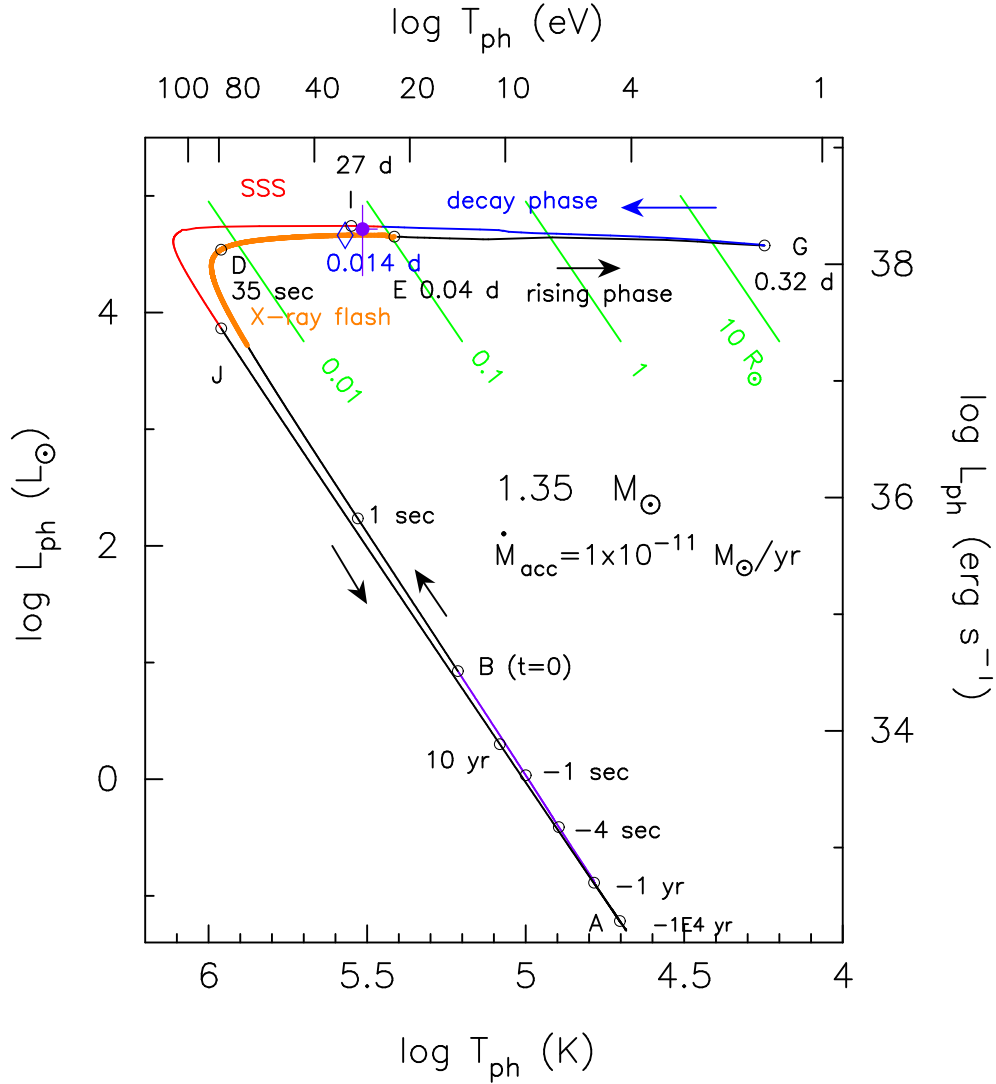


Figure 2. The H-R diagram of one cycle of hydrogen shell flashes for our nova outburst model of a $1.35 M_{\odot}$ WD with the mass accretion rate of $\dot{M}_{\text{acc}} = 1 \times 10^{-11} M_{\odot} \text{ yr}^{-1}$, taken from Figure 1(a) of M. Kato et al. (2025) with several modifications. Only the photospheric luminosity L_{ph} and temperature T_{ph} of the exploding WD are plotted. Note that the contributions from those outside the WD photosphere, e.g., the WD winds (ejecta), irradiated disk, and companion star, are not included. Selected stages during a shell flash are denoted counterclockwise direction starting from the bottom of the cycle. A: quiescent phase before the shell flash. B: the epoch when L_{nuc} reaches maximum ($t = 0$). D: the peak of soft X-ray luminosity L_{X} (0.3–1.0 keV). E: winds emerge from the photosphere. G: the maximum expansion of the photosphere and maximum wind mass loss rate. The straight green lines depict the locus of constant photospheric radius of $R_{\text{ph}} = 10, 1, 0.1, \text{ and } 0.01 R_{\odot}$. The times at selected stages are indicated before and after stage B. The open blue diamond labeled “0.014 d” indicates the epoch of the first ASAS-SN detection of the V1674 Her outburst in Figure 1. The filled purple circle with error bars indicates the detection of YZ Ret in the X-ray flash phase (O. König et al. 2022). See Figure 1(a) of M. Kato et al. (2025) for more details and other symbols.

in Section 2. Then, we introduce our binary model that consists of a hot and bright WD, an irradiated accretion disk and companion star in Section 3. We compare our model light curves with observational results of V1674 Her in Section 4. Discussion and conclusions follow in Sections 5 and 6, respectively.

2. BASIC NOVA MODEL

2.1. H-R Diagram of one cycle of the nova outburst

Figure 2 shows one cycle in the H-R diagram of the nova outburst calculated by M. Kato et al. (2025), i.e., a $1.35 M_{\odot}$ WD with a mass accretion rate of $1 \times 10^{-11} M_{\odot} \text{ yr}^{-1}$. This plot is essentially the same as Figure 1(a) of M. Kato et al. (2025) with several modifications. In the quiescent phase (inter-outburst period), the accreting WD stays around the bottom of the loop. After a ther-

mononuclear runaway starts, the WD moves quickly upward keeping the photospheric radius almost constant. We define the origin of time (stage B, $t = 0$) by the epoch when the nuclear energy generation rate reaches maximum, $L_{\text{nuc}} = L_{\text{nuc}}^{\text{max}}$. After that, the photospheric temperature continuously increases to its maximum at $\log T_{\text{ph}}^{\text{max}}$ (K) = 6.02. With such a high temperature, the WD photosphere emits soft X-ray photons, which is called the X-ray flash phase. Then, the WD envelope expands and the photospheric temperature turns to decrease.

The epoch of the first optical detection of the V1674 Her outburst (ASAS-SN $g = 17.0$ on day 0.014, R. M. Quimby et al. 2024) is plotted by the open blue diamond labeled “0.014 d” on the H-R track.

Optically thick winds emerge from the WD photosphere when the envelope expands and the photospheric temperature decreases to $\log T_{\text{ph}}$ (K) = 5.41 (stage E, the open circle labeled E). Soft X-rays could be absorbed by wind itself far outside the photosphere, thus, we regard this to be the end epoch of the X-ray flash phase.

We showed the part of X-ray flash phase with the orange line on the track, that is, from the epoch of $L_X = 10^{3.2} L_{\odot}$ ($= 0.1 L_X^{\text{max}}$) to stage E.

The photosphere further expands and reaches maximum at stage G. The wind mass loss rate also increases and reaches maximum at the same time at stage G. The hydrogen-rich envelope quickly loses its mass mainly due to wind mass loss. After stage G, the photosphere turns to shrink with time while the photospheric temperature turns to increase. The optically thick winds stop at epoch I when the photospheric temperature increases to $\log T_{\text{ph}}$ (K) = 5.55. The WD emits soft X-ray photons (the supersoft X-ray source (SSS) phase). As hydrogen burning decays, the WD becomes faint and returns to the quiescent phase (the bottom of the loop).

In the present work, we focus on a very early phase of the outburst, i.e., from stage B ($t = 0$) to the X-ray flash phase (orange line part on the H-R track), and to the ensuing rising phase (black line part) of the WD.

2.2. Free-free emission model V light curve

After the optically thick winds emerge from the photosphere, we have calculated free-free emission luminosity from the optically thin ejecta outside the photosphere (e.g., I. Hachisu & M. Kato 2006; I. Hachisu et al. 2020). While optically thick winds are accelerated deep inside the photosphere, the nova wind itself becomes optically thin outside the photosphere. The V luminosity can be simplified as

$$L_{V,\text{ff},\text{wind}} = A_{\text{ff}} \frac{\dot{M}_{\text{wind}}^2}{v_{\text{ph}}^2 R_{\text{ph}}}, \quad (1)$$

where \dot{M}_{wind} , v_{ph} , and R_{ph} are the wind mass loss rate, wind velocity at the photosphere, and photospheric radius, respectively, calculated by M. Kato et al. (2025). See Equation (3) in M. Kato et al. (2025) for details on the coefficient A_{ff} and how to determine it for V1674 Her.

We depict the calculated $L_{V,\text{ff},\text{wind}}$ (free-free emission luminosity) by the black line in Figure 1 based on M. Kato et al. (2025)’s nova evolution calculation. It is remarkable that only the free-free emission model V light curve reasonably reproduces the entire nova g/V light curve in the wind phase, from a very early phase of $g = 15$ mag (at 0.078 day) until $V = 13.3$ mag (on day 22.4). Here, we assume that $g - V = 0$ (R. M. Quimby et al. 2024), and adopt the V band distance modulus toward V1674 Her of $\mu_V \equiv (m - M)_V = 16.3$, distance of $d = 8.9$ kpc, and extinction of $E(B - V) = 0.5$ after M. Kato et al. (2025).

The wind phase begins at 0.04 day and ends on day 26. Almost throughout this interval, the free-free emission model V light curve reasonably reproduces the observed g/V light curve from $g = 15.0$ to $V \sim 13$. This indicates that the optical contribution from each photosphere of the disk, companion star, or WD is negligible from $g = 15.0$ (at 0.078 day) to $V = 13.3$ (on day 22.4).

2.3. X-ray flash phase

As introduced in Section 1, the first detection data of ASAS-SN (open blue diamonds at $t = 0.014$ day in Figure 1) was obtained much earlier than when our free-free emission model V light curve (black line) rises up. This epoch ($t = 0.014$ day) corresponds to the X-ray flash phase, as shown by the open blue diamond in the H-R diagram (Figure 2). It is interesting that this position is very close to that of YZ Ret during its X-ray flash phase in the H-R diagram, of which the temperature and luminosity are estimated by O. König et al. (2022). YZ Ret is a very fast nova of which the WD mass is estimated to be very massive ($> 1.3 M_{\odot}$, M. Kato et al. 2022b,c). This resemblance also suggests that the ASAS-SN $g = 17.0$ data was obtained during its X-ray flash phase. In the X-ray flash phase, the hydrogen-rich envelope of the WD is too hot ($T_{\text{ph}} \sim 3 \times 10^5$ K) to be bright in optical. This leads us to include the brightnesses of an accretion disk and companion star irradiated by the hot and bright WD. In what follows, we will see whether or not the irradiated disk and companion star are enough to reproduce these g band brightnesses of $g = 17.0$ – 16.2 on day 0.014–0.017.

3. BINARY MODEL

3.1. Binary parameters

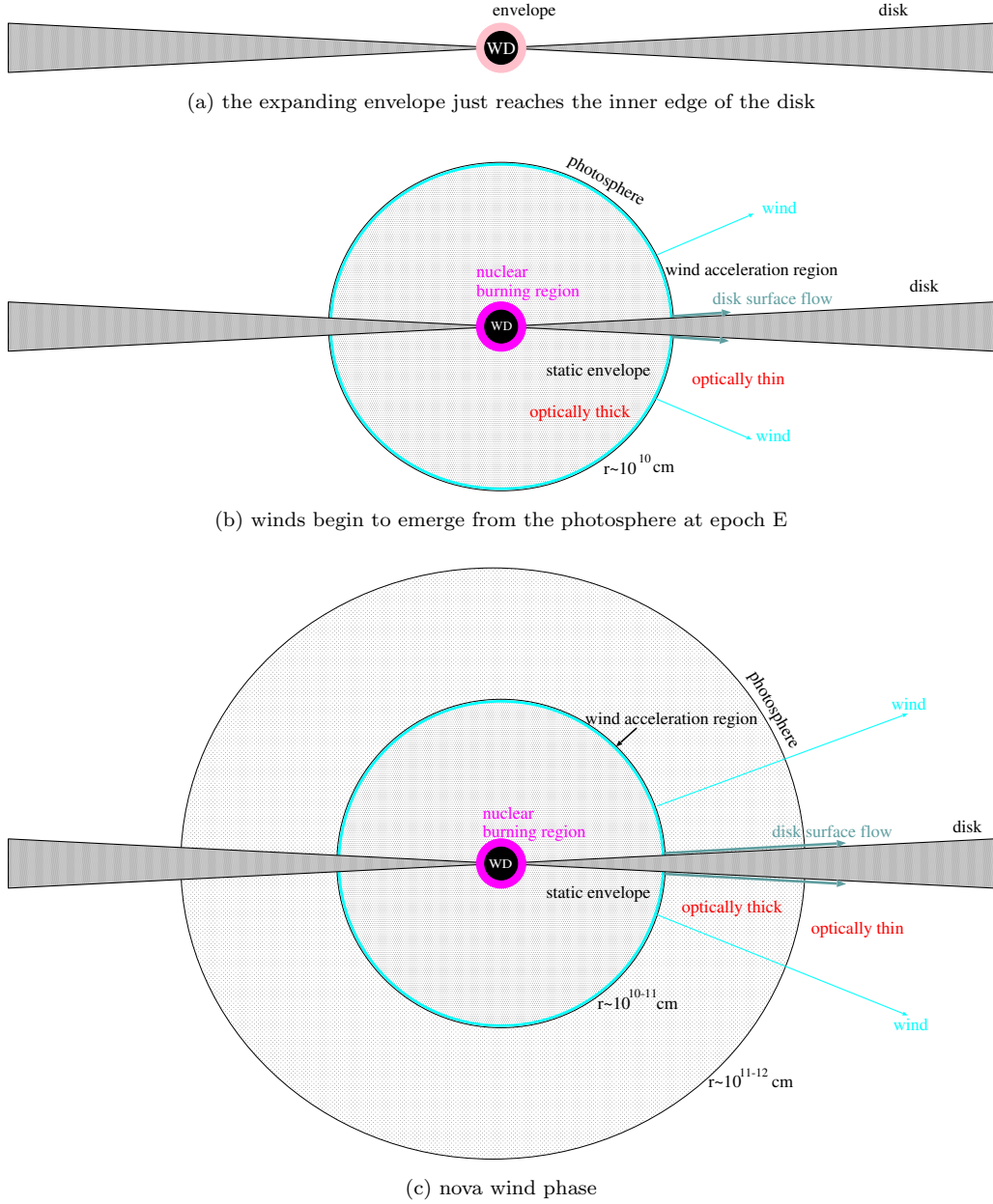


Figure 3. Schematic configurations of a WD envelope and accretion disk during a nova outburst. (a) In the X-ray flash phase: when the expanding envelope reaches the inner edge of the accretion disk. (b) At epoch E: The optically thick winds emerge from the photosphere. The accretion disk is not disrupted and the winds blow avoiding the region of the disk. (c) Early wind phase after stage E: The disk has not been totally engulfed yet by the WD envelope. The critical point of wind acceleration is at $R_{\text{cr}} \approx 0.2 R_{\odot}$. Optically thick winds have an opening angle avoiding the accretion disk. The disk surface flow occurs owing to the Kelvin-Helmholtz instability or friction between the winds and the disk surface. The spherical nova envelope configurations are taken from the spherically symmetric $1.35 M_{\odot}$ WD model (M. Kato et al. 2025). The thick light-cyan region describes the acceleration region of winds. The dark-cyan arrows represent the disk surface (boundary layer) flows, which exist near the surface of accretion disk and have slower outflow velocities than those of winds. Here, we neglect the inner magnetic polar accretion region/stream because they are embedded by the almost static hydrogen-rich envelope rather inside the acceleration region.

Our binary model consists of a $1.35 M_{\odot}$ WD (M. Kato et al. 2025), accretion disk, and companion star. Both accretion disk and companion star are irradiated by the hot and bright WD. We adopt a companion mass of $M_2 = 0.26 M_{\odot}$ after R. M. Quimby et al. (2024), the orbital period of 0.15291 day ($= 3.67$ hr) and ephemeris of Minimum Light $= \text{HJD } 2,459,400.637 + 0.15291 E$ after J. Patterson et al. (2022). We assume that the epoch of minimum light corresponds to the configuration that the companion star is just in front of the WD. Then, we obtain the separation of $a = 1.41 R_{\odot}$, the effective Roche lobe radii of $R_{\text{RL},1} = 0.739 R_{\odot}$ and $R_{\text{RL},2} = 0.351 R_{\odot}$, and the orbital velocities of $v_1 = 75.4 \text{ km s}^{-1}$ and $v_2 = 391 \text{ km s}^{-1}$. The inclination angle of the binary/accretion disk is assumed to be $i = 67^{\circ}$ after G. R. Hacht et al. (2024). Among above parameters, only the inclination angle is not well constrained, so we calculated with other two inclination angles of $i = 45^{\circ}$ and $i = 75^{\circ}$ to examine the brightness variation.

3.2. Disk is not disrupted

Theoretically, we expect that the accretion disk remains undisrupted during the nova outburst. As already explained in Section 1, the WD envelope expands almost hydrostatically during the X-ray flash phase. In our nova model, the photosphere of expanding envelope reaches the inner edge of the accretion disk, e.g., at $t = 5.3 \text{ min}$ ($= 0.0036 \text{ day}$). Here, we assumed the inner edge of the disk to be $R_{\text{in}} \approx 0.02 R_{\odot}$ after R. M. Quimby et al. (2024) for the intermediate polar (IP) V1674 Her. The disk is almost intact because optically thick winds do not yet emerge from the photosphere, as illustrated in Figure 3(a).

After that, the WD photosphere continues to expand keeping a hydrostatic balance. The inner disk is engulfed by the envelope, but not disrupted because the envelope is in hydrostatic equilibrium and its density is much smaller than that of the accretion disk. The optically thick winds begin to blow from the WD photosphere ($R_{\text{ph}} \approx 0.1 R_{\odot}$) on day 0.04 (stage E). The acceleration region appears close to the photosphere as shown in Figure 3(b) (thick light-cyan region). A part of the disk surface could be blown in the wind, the flow of which occurs only outside the acceleration region. We call such a relatively dense flow “the disk surface flow” (I. Hachisu et al. 2025). The velocity of the disk surface flow is slower than the nova wind.

Figure 3(c) illustrates a successive phase. The photosphere of nova winds expands faster leaving the acceleration region behind, the position of which is far inside the photosphere. Because the density of the WD envelope is much lower than that of the accretion disk, the

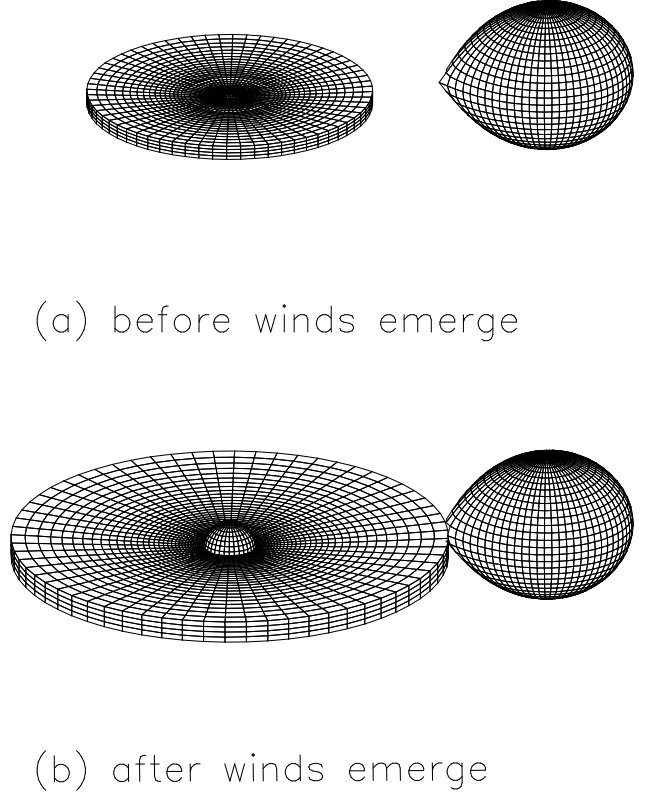


Figure 4. Geometric configuration models of our disk and companion star in Figure 5(a). The masses of the WD and Roche-lobe-filling companion star are $1.35 M_{\odot}$ and $0.26 M_{\odot}$, respectively. The orbital period is $P_{\text{orb}} = 0.1529 \text{ day}$ ($= 3.67 \text{ hr}$). The inclination angle of the binary is $i = 67^{\circ}$. The separation is $a = 1.41 R_{\odot}$ while their effective Roche lobe radii are $R_{\text{RL},1} = 0.739 R_{\odot}$ and $R_{\text{RL},2} = 0.351 R_{\odot}$. We assume, in panel (a), the disk size is $R_{\text{disk}} = 0.628 R_{\odot}$ ($= 0.85 R_{\text{RL},1}$), the height of the disk edge to be 0.05 times the disk size but, in panel (b), the disk size is $R_{\text{disk}} = 0.961 R_{\odot}$ ($= 1.3 R_{\text{RL},1}$) and the edge height is 0.05 times the disk size. The photospheric surfaces of the disk and companion star are irradiated by the central hot WD. Such irradiation effects are all included in the calculation of the V light curve reproduction (see Hachisu & Kato 2001, for the partition of each surface and calculation method of irradiation). We also include the effect of viscous heating in the accretion disk for a given mass-accretion rate (Hachisu & Kato 2001). We neglect the inner edge of the disk mainly because the optical brightness is determined by the surface area of the disk and a central hole (very small area) hardly contributes to the optical brightness.

nova winds are expanding almost spherically but avoid the equatorial region shaped by the dense disk as illustrated in Figure 3(b) and (c).

Before the wind blows, i.e., in the stage around Figure 3(a), the total emission from the binary consists of the photospheric emission (WD photosphere + irradiated accretion disk photosphere + companion star pho-

tosphere), although the companion star is not depicted in these plots. After the winds blow (Figure 3(b) and (c)), the total emission from the binary consists of the photospheric emission and free-free emission from the nova wind.

3.3. Irradiated disk and companion star

In the very early phase of the outburst, the irradiated disk photosphere and companion star photosphere dominantly contribute to the optical luminosity of V1674 Her. In our calculation, we simply assume that the companion star fills its inner critical Roche lobe, as depicted in Figure 4. We assume different size and shape of the accretion disk before and after the nova wind emerges from the photosphere.

We first assume that the disk surface is cylindrically symmetric around the WD. Then, the outer size of the disk is defined by

$$R_{\text{disk}} = \alpha R_{\text{RL},1}, \quad (2)$$

and the height of the disk at the outer edge is given by

$$H_{\text{disk}} = \beta R_{\text{disk}}. \quad (3)$$

The surface height z of the disk at the equatorial distance $\varpi = \sqrt{x^2 + y^2}$ from the center of the WD is assumed to be

$$z = \left(\frac{\varpi}{R_{\text{disk}}} \right) H_{\text{disk}}. \quad (4)$$

Before the nova wind blows, we adopt $\alpha = 0.85$ and $\beta = 0.05$ as in Figure 4(a), where $\alpha = 0.85$ is close to the tidal limit of the disk (see, e.g., Muraoka et al. 2024). After the nova wind blows, we adopt $\alpha = 1.3$ and $\beta = 0.05$ as in Figure 4(b). This value is taken after Muraoka et al. (2024) who found that the optically thick part of the disk is extended up to $\alpha \sim 1.3$ during the nova wind phase in the 2021 outburst of U Sco. We interpret that a large size disk over the tidal limit is a manifestation of the photosphere of the disk surface flow (optically thick part). It is reasonable that we assume axisymmetric flow for the disk surface flow when the nova wind is axisymmetric, i.e., almost spherically symmetric (see, e.g., I. Hachisu et al. 2025, for more details).

We partition each photosphere of the WD, disk, and companion star into many sectors (or patches) as in Figure 4. Each small patch absorbs high energy photons from the WD. The photospheric temperature of each patch increases. We assume that the photosphere of each patch emits blackbody photons at this increased temperature. The V light curve is calculated from the summation of each patch with the standard V filter response function. See Hachisu & Kato (2001) for the

partitioning of each surface and calculation method of irradiation. Note that, in Figure 4, gas is optically thin outside the mesh surfaces (i.e., photospheres of the disk, WD, and companion star). In our irradiation calculation, we neglect absorption by optically thin gas outside the mesh surfaces.

As introduced in Section 3.2, V1674 Her is an IP (J. Patterson et al. 2022). The inner edge R_{in} of the disk is determined by the Alfvén radius where the ram pressure of the inflowing gas balances with the magnetic force of the WD (e.g., Equation (2) of R. M. Quimby et al. 2024, $R_{\text{in}} \sim 0.02 R_{\odot}$ for typical values). We neglect this central hole of the accretion disk in our luminosity calculation of the irradiated disk, because the optical brightness of the accretion disk depends on the surface area of the disk and a small innermost hole hardly contributes to the optical brightness of the disk.

We include the effect of viscous heating by mass accretion through the accretion disk (see Hachisu & Kato 2001, for details on this effect). As the mass accretion increases, the temperatures of the disk surface increases and, as a result, the disk brightens up. R. M. Quimby et al. (2024) showed that the pre-outburst brightness of V1674 Her gradually increased up to $g = 19.17$, 1.7 days before the outburst, from the Zwicky Transient Facility (ZTF) archive data (see the trend from 2019 to 2021 in Figure 5(a)). To reproduce $g = 19.2$ before the outburst, we assume a mass accretion rate to be as high as $\dot{M}_{\text{acc}} = 2 \times 10^{-7} M_{\odot} \text{ yr}^{-1}$.

3.4. Composite light curves

The V magnitude luminosity from the WD photosphere $L_{V,\text{ph},\text{WD}}$ is calculated from the blackbody emission with standard V response function. The V luminosity from each photosphere is the summation of the photospheric emission from the WD, irradiated accretion disk surface, and the irradiated companion, which is expressed by

$$L_{V,\text{ph}} = L_{V,\text{ph},\text{WD}} + L_{V,\text{ph},\text{disk}} + L_{V,\text{ph},\text{comp}}. \quad (5)$$

After optically thick winds emerge from the WD photosphere, free-free emission from the optically-thin ejecta outside the WD photosphere begins to contribute to the V luminosity. We have calculated the composite V light curve as

$$L_{V,\text{total}} = L_{V,\text{ff},\text{wind}} + L_{V,\text{ph},\text{WD}} + L_{V,\text{ph},\text{disk}} + L_{V,\text{ph},\text{comp}}, \quad (6)$$

where $L_{V,\text{total}}$ is the total V luminosity of the V1674 Her system, $L_{V,\text{ff},\text{wind}}$ the free-free emission V luminosity.

Figure 5(a) shows each component separately, $L_{V,\text{ph}}$ (Equation (5): thick orange line) and $L_{V,\text{ff},\text{wind}}$ (Equa-

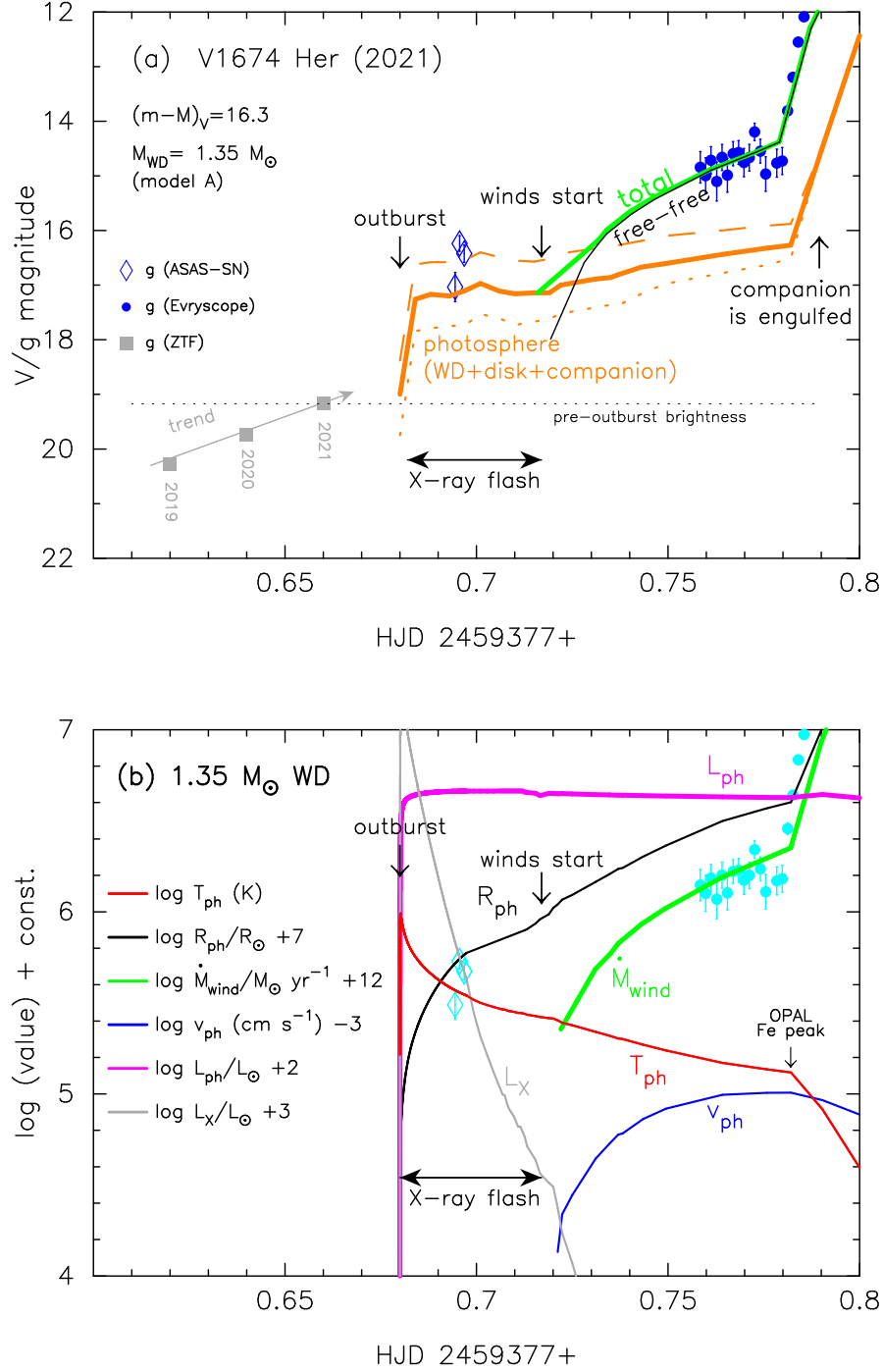


Figure 5. (a) Comparison of our theoretical V light curve with observational data in the first 0.12 days of the V1674 Her 2021 outburst. We assumed the origin of time ($t = 0$) to be JD 2,459,377.68. The three orange lines (thick solid, dashed, and dotted) correspond to the photospheric V light curves of the binary with three different inclination angles of $i = 67$, 45 , and 75° , respectively. The black line shows the free-free emission model V light curve and the green line is the total V luminosity of free-free (black line) and photospheric (thick solid orange line) luminosities. Blue filled circles and blue open diamonds show Evryscope and ASAS-SN g magnitudes, respectively. The data are all taken from R. M. Quimby et al. (2024). The epoch when the companion star is engulfed by the WD photosphere is indicated by the upward arrow for our WD model. A brightening trend of the Zwicky Transient Facility (ZTF) g magnitudes in the pre-outburst phase is shown by the filled gray squares and the arrow penetrating them. Note that its timescale is very different from that of abscissa, in units of year. (b) Various photospheric properties of our $1.35 M_{\odot}$ WD model are plotted during the same interval as in panel (a). The data are all taken from M. Kato et al. (2025).

tion (1): thin black line) as well as the total emission $L_{V,\text{total}}$ (Equation (6): thick green line).

The downward arrow labeled “winds start” indicates the epoch when the nova wind emerges from the photosphere. Before this epoch, the irradiated disk and companion star are the main optical sources. After winds emerges, free-free emission dominates as shown by the green and black lines.

4. X-RAY FLASH PHASE LIGHT CURVE OF V1674 HER

Figure 5(a) shows the earliest optical light curve, the V luminosity of which is contributed mainly by the accretion disk and companion star photospheres (thick orange line). It is soon replaced by free-free emission from the optically-thin ejecta (thin black line) after nova winds emerge from the WD photosphere. Figure 5(b) shows the $1.35 M_{\odot}$ WD properties, i.e., the photospheric luminosity L_{ph} , X-ray luminosity (0.3 - 1.0 keV) L_{X} , temperature T_{ph} , radius R_{ph} , velocity v_{ph} , and wind mass-loss rate \dot{M}_{wind} . The X-ray flux (gray line) sharply rises just after the onset of thermonuclear runaway, $t_{\text{OB}} = \text{HJD } 2,459,377.68$, followed by a slower decline. We depict the X-ray flash phase by the horizontal two-headed black arrow. We see that the ASAS-SN g data are obtained exactly during the X-ray flash phase. The V luminosity is dominated by the irradiated accretion disk and companion star (thick orange line). In other words, the ASAS-SN g data is the first optical detection of an X-ray flash.

In what follows, we describe details of our V light curve model step by step.

4.1. Mass accretion rate on to the white dwarf

R. M. Quimby et al. (2024) showed that the pre-outburst brightness of V1674 Her gradually increased up to $g = 19.17$, until 1.7 days before the outburst, from the ZTF archive data (see the trend from 2019 to 2021 in Figure 5(a)). The reason of the gradual brightening is unknown. If we attribute this brightening to that of the accretion disk, we need a mass accretion rate on to the WD as high as $\dot{M}_{\text{acc}} = 2 \times 10^{-7} M_{\odot} \text{ yr}^{-1}$. In other words, the disk with such a high mass accretion rate is as bright as $V \sim 19$ owing to viscous heating.

This high mass accretion rate on to the WD through the accretion disk, $\dot{M}_{\text{acc}} = 2 \times 10^{-7} M_{\odot} \text{ yr}^{-1}$, is consistent with M. Kato et al. (2025)’s analysis. V1674 Her shows a longer SSS phase than the expected interval if no mass accretion occurs during the outburst. They showed that the observed long SSS phase can be reproduced if such a high mass accretion as $\dot{M}_{\text{acc}} \sim 3 \times 10^{-7} M_{\odot} \text{ yr}^{-1}$ had continued during the outburst because much

fresh fuel is supplied to hydrogen burning. Otherwise, its duration is too short to be compatible with the observation.

4.2. More than 2 mag brightening-up after hydrogen burning

Just after the nova outburst begins, the photospheric brightness (thick solid orange line) increases/jumps up from $g = 19.2$ to $g = 17.0$ mag. The pre-outburst magnitude of $g = 19.2$ is owing to the viscous-heating accretion disk whereas $g = 17.0$ mag is from the irradiated disk and companion star. A similar phenomenon of binary brightening-up of ~ 2 mag or more was first definitely pointed out by I. Hachisu & M. Kato (2025). They proposed a demarcation criterion how to distinguish if hydrogen-burning is on/off on a WD for millinova outbursts (P. Mróz et al. 2024). V1674 Her provides another example that hydrogen burning on the WD makes ΔV (or Δg) ~ 2 mag increase in the disk brightness.

4.3. From photospheric emission to free-free emission

Figure 6 depicts our summary of light curves for the 2021 outburst of V1674 Her, which combines Figure 1 with Figure 5(a). In the earliest phase before the wind starts, the light curve can be explained by the emission from the irradiated photospheres of the disk and companion star. After the winds start, the free-free emission model V light curve well follows the Evryscope data (blue filled circles) from the first data of $g = 14.844$ (0.0784 day) until the last pre-maximum data of $g = 7.102$ (0.2791 day) over 7 magnitudes rise including a break of slope at $g = 14.3$ (0.1 day), where we assumed $V - g = 0$. This excellent agreement with the model and observation implies that, in the rising phase from $g = 14.9$ to $g = 7.1$, there is no contribution of other sources such as a shocking power.

5. DISCUSSION

5.1. Two-step rise in the free-free emission light curve

Figure 5(a) shows that our free-free model V light curve (black line) well follows the temporal variation of the Evryscope g light curve (blue filled circles) including before and after the break of slope on HJD 2,459,377.78. This sudden rise in the g magnitude is theoretically explained as follows: The flux of free-free emission depends strongly on the wind mass-loss rate, i.e., $L_{V,\text{ff,wind}} \propto (\dot{M}_{\text{wind}})^2$ from Equation (1), which suddenly increases at the break.

This sudden change of the wind mass loss rate is closely related to the interior structure of the nova envelope. Figure 7(a) plots the opacity κ distributions

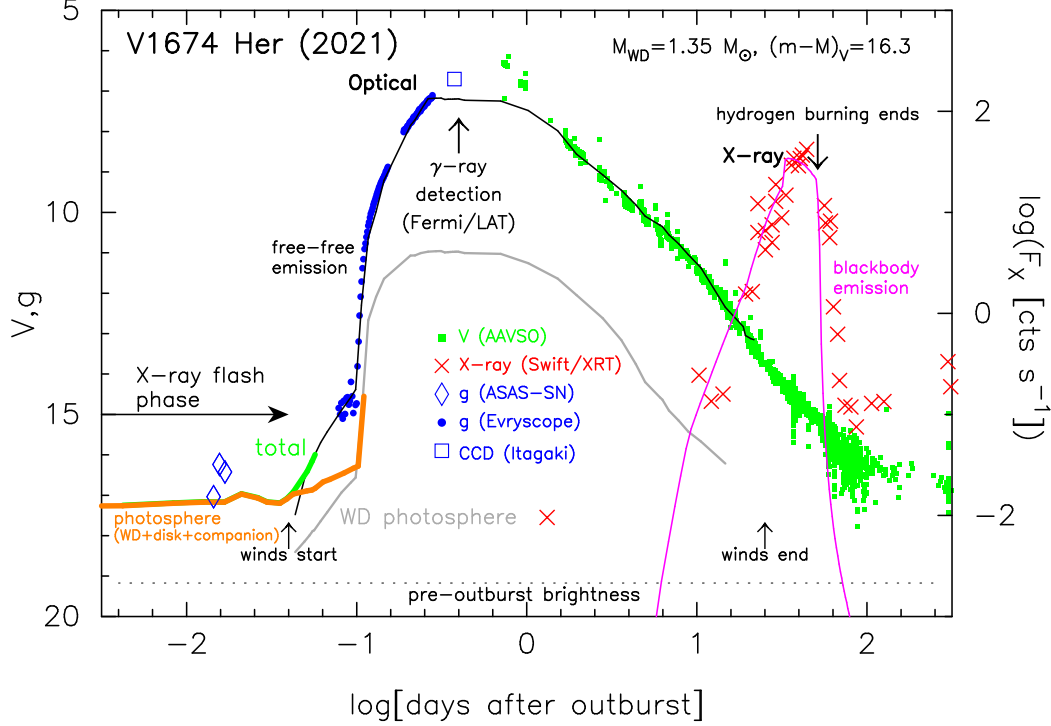


Figure 6. Same as Figure 1, but we added our light curve model (thick orange line) of the irradiated accretion disk and companion star including the WD photosphere (light-gray line). We also add the total flux (thick green line) of the free-free emission (black line) plus photospheric blackbody emission (thick orange line). The V luminosity of the WD photosphere is much smaller than that of the free-free emission luminosity.

(OPAL, C.A. Iglesias & F.J. Rogers 1996) in the envelope against the temperature for three stages, slightly before (magenta line) and after (black line) the epoch of the break, and at the maximum expansion of the WD photosphere (green line), stage G. There are small and large opacity peaks, which correspond to the ionization zone of C/O, Fe, and He, from inside to outside (from high temperature to low temperature). The right edge of each line corresponds to the photosphere. In an early stage (the magenta line in Figure 7(a)) before the g magnitude break, the photospheric temperature is so high and the photosphere is inside the strong Fe peak. In a later stage (the black line in Figure 7(a)) after the g magnitude break, the envelope has expanded so that the photospheric temperature decreases down outside the Fe peak. This difference causes weak (before) and strong (after) acceleration of winds.

We plot the distributions of the photon luminosity L_r and local Eddington luminosity defined by

$$L_{\text{Edd},r} \equiv \frac{4\pi c G M_{\text{WD}}}{\kappa}, \quad (7)$$

where L_r the photon diffusive luminosity at the radius r from the WD center, $L_{\text{Edd},r}$ is the local Eddington luminosity at the radius r , and the opacity κ is a function of the density and temperature, c the speed of light,

and G the gravitational constant. Figure 7(b) depicts the L_r (black line) and $L_{\text{Edd},r}$ (red line) distributions slightly before the break, corresponding to the magenta line in Figure 7(a), while Figure 7(c) plots the distributions slightly after the break, corresponding to the black line in Figure 7(a).

The optically thick winds are accelerated by radiative pressure gradient/difference deep inside the photosphere (M. Friedjung 1966; M. Kato & I. Hachisu 1994). The radiation pressure gradient/difference is simply written by $\Delta P_{\text{rad}} \propto (L_r - L_{\text{Edd},r})$ for a local super-Eddington region of $L_r - L_{\text{Edd},r} > 0$. Here, P_{rad} is the radiation pressure. We see in Figure 7(b) and (c) that the difference of $L_r - L_{\text{Edd},r}$ sharply increases as the envelope expands and reaches maximum at the break. The break occurs just at the photospheric temperature of $\log T_{\text{ph}} (\text{K}) \sim 5.2$, as shown by the red line in Figure 5(b). This corresponds to the temperature at the Fe peak of the opacity κ as in Figure 7(a). After the break (at $\log T_{\text{ph}} (\text{K}) \sim 5.2$), the difference, $L_r - L_{\text{Edd},r}$, gradually increases always keeping the Fe peak of κ inside the photosphere. Comparing the difference between before (Figure 7(b)) and after (Figure 7(c)) the break, the acceleration force of the wind simply increases by a factor of several. This is the reason of sudden increase of the wind mass loss rate and thus, sudden increase of the

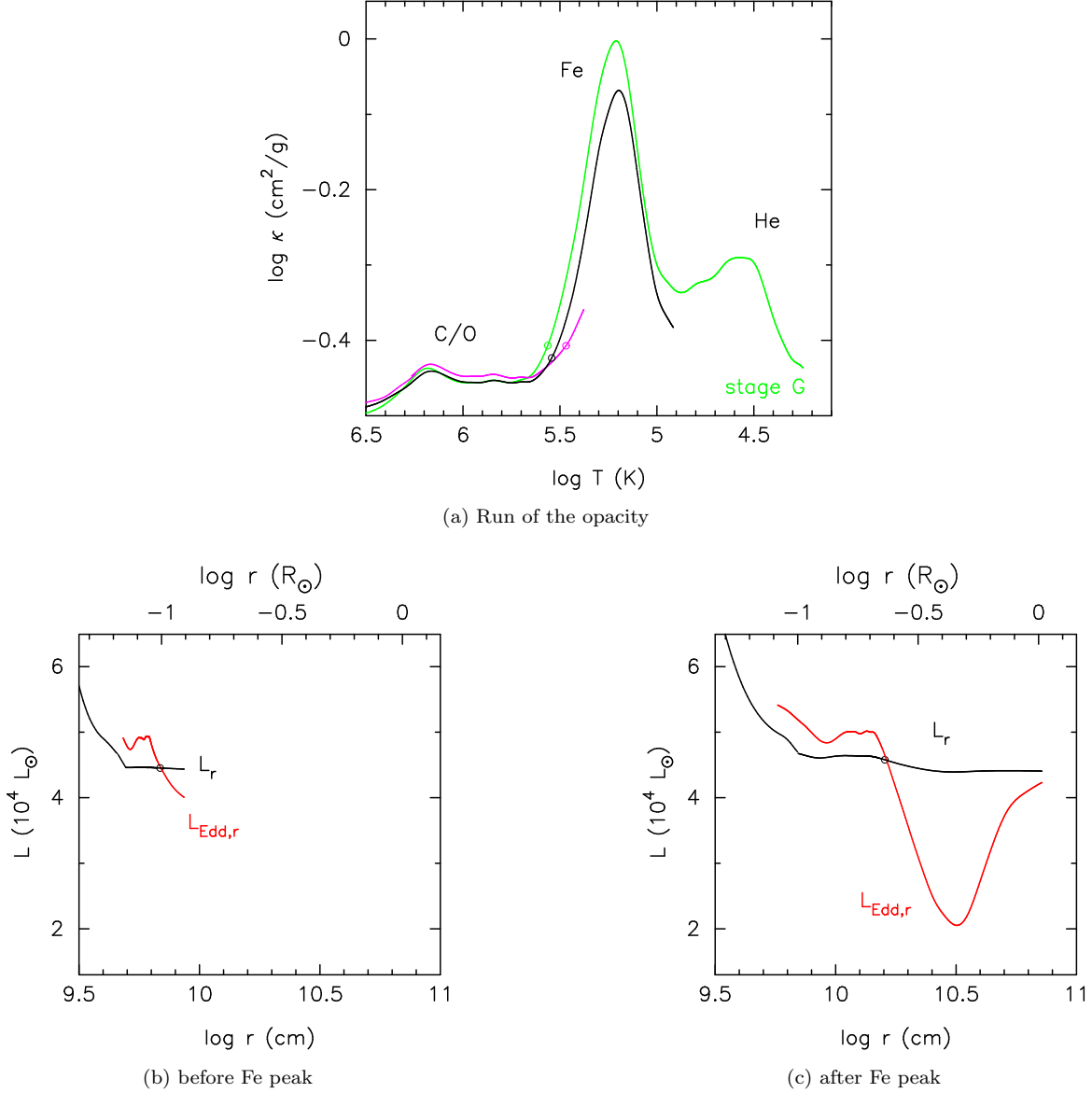


Figure 7. (a) Run of the radiative opacity against the temperature from inside to outside in our $1.35 M_\odot$ WD for three stages. The open circles on each line correspond to the critical points of Parker type steady-state wind solutions (M. Kato & I. Hachisu 1994). Matter is sharply accelerated around this critical point. Magenta line: The stage of $\log T_{\text{ph}}(\text{K}) = 5.38$ (at $t = 0.045$ day). All the envelope still lies inside the Fe peak ($\log T \approx 5.2$) of the opacity. Black line: The stage of $\log T_{\text{ph}} = 4.92$ (at $t = 0.11$ day). The envelope expands to include the Fe opacity peak and its photosphere is outside the peak. Green line: stage G at the maximum expansion of the photosphere (at $t = 0.32$ day) in Figure 2. (b) The diffusive luminosity L_r and local Eddington luminosity $L_{\text{Edd},r}$ are plotted against the radius r for the stage of magenta line in panel (a). The open circle corresponds to the critical point of Parker type supersonic wind. (c) Same as panel (b), but for the stage of the black line in panel (a).

rising slope in the free-free emission light curve at/near $\log T_{\text{ph}} \text{ (K)} \sim 5.2$.

R. M. Quimby et al. (2024) noted that the early Evryscope g data indicate a shallow dip between the slow and fast rises which does not appear in M. Kato et al. (2025)’s model as shown in Figure 5(a). If this optical dip is real, it would suggest that a rapid structure change near the photosphere can not be followed by the

numerical method of Kato et al. who adopted a steady-state wind approximation for each time step.

5.2. Inclination angle of the binary

We assumed the inclination angle $i = 67^\circ$ in our calculation of the light curve. The resultant brightness of $V \sim 17$ is consistent with the first ASAS-SN observation of $g = 17.0$ at $t = 0.0144$ day (HJD 2,459,377.6944) as shown in Figure 5(a). Slightly (~ 105 and 210 s) later,

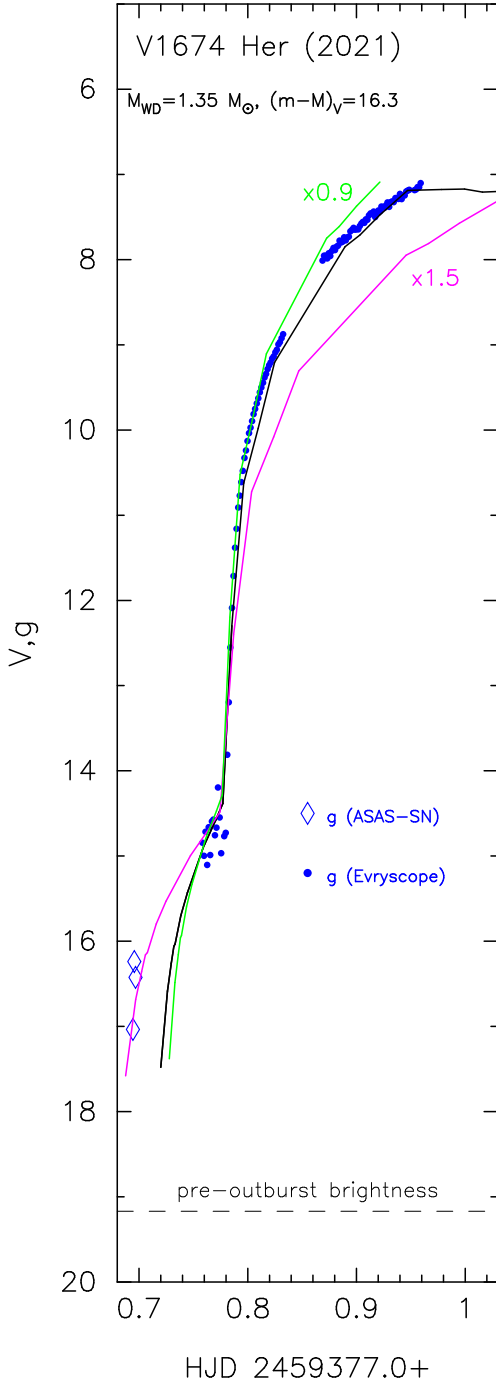


Figure 8. The g band light curves (blue symbols) and our free-free emission model V light curve (black line) in the very early phase of the V1674 Her outburst. The observational data and free-free emission model V light curve (black line) are the same as those in Figure 6. We add other two model light curves (magenta and green lines), the timescales of which is 1.5 and 0.9 times longer than that of the original model light curve (black line). We nail down each break of the light curves on HJD 2,459,377.78. The wind phase of magenta line starts just at the first ASAS-SN detection.

the g magnitude brightens up to $g = 16.24$ ($t = 0.0156$ day) and $g = 16.42$ ($t = 0.0168$ day).

This short interval is consistent with the timescale of spin period of the WD, $P_{\text{spin}} = 501$ s, as discussed by R. M. Quimby et al. (2024). However, the WD photosphere has already expanded up to $R_{\text{ph}} \sim 0.05 R_{\odot}$ at $t = 0.0144$ day ($= 21$ min) and has completely engulfed the magnetic funnels of the innermost region of the accretion disk if the inner edge of the disk is as small as $R_{\text{in}} \sim 0.02 R_{\odot}$ (a typical value of Equation (2) in R. M. Quimby et al. 2024). So, it is unlikely that this very short timescale variation is related to the spin of the WD unless R_{in} is as large as $\gtrsim 0.06 R_{\odot}$. Such a larger hole in the disk could be possible for some extreme cases for V1674 Her. Substituting the WD mass of $M_{\text{WD}} = 1.35 M_{\odot}$, mass accretion rate of $\dot{M}_{\text{acc}} = 2 \times 10^{-7} M_{\odot} \text{ yr}^{-1}$, and magnetic field of $B = 10^7$ G into Equation (2) of R. M. Quimby et al. (2024), we obtain $R_{\text{in}} \approx 0.056 R_{\odot}$. Or substituting $1.35 M_{\odot}$, $\dot{M}_{\text{acc}} = 1 \times 10^{-11} M_{\odot} \text{ yr}^{-1}$, and $B = 10^5$ G, we have $R_{\text{in}} \approx 0.069 R_{\odot}$. If it is the case, this short timescale variation could be explained by some geometric effect of the disk and magnetic funnels, as suggested by R. M. Quimby et al. (2024).

When $R_{\text{in}} \lesssim 0.05 R_{\odot}$, we do not know the origin of this short timescale variability. Because the first data has relatively large statistic error of $\sigma_g = 0.3$ mag, we searched other model light curves that fit the second and third data by changing the inclination angle of the binary. As shown in Figure 5(a), a smaller inclination angle of $i = 45^\circ$ (dashed orange line) makes magnitude 0.5 mag brighter than the $i = 67^\circ$ case (thick solid orange line) that is broadly consistent with the ASAS-SN $g = 16.4$ magnitudes. Assuming that the second and third data are securer than the first one, we prefer to the inclination angle of $i = 45^\circ$ rather than $i = 67^\circ$.

5.3. Timescale of the optical rise

The earliest ASAS-SN g data were obtained in the X-ray flash phase of V1674 Her as shown in Figure 5. Here, we discuss another possibility that the ASAS-SN data were explained by the free-free emission light curve, not by the irradiation effect of a disk in the X-ray flash phase.

The most important parameters for the light curve fitting is the WD mass. M. Kato et al. (2025) presented only two light curves of $1.35 M_{\odot}$ WD with the mass accretion rate of $\dot{M}_{\text{acc}} = 1 \times 10^{-11} M_{\odot} \text{ yr}^{-1}$ (model A) and $5 \times 10^{-10} M_{\odot} \text{ yr}^{-1}$ (model B). Although they claimed they did not intend to make a fine tuning model, their model with the lower mass accretion rate happens to show an excellent agreement with the V1674 Her

light curve data, both in the fast rising phase and decay phase. If they adopt a massive (less massive) WD, the light curve will be faster (slower) and does not match the observation. Therefore, we conclude that $1.35 M_{\odot}$ is a quite good WD mass for V1674 Her.

The second important parameter is the mass accretion rate. If we adopt a larger (smaller) mass accretion rate, the rising phase becomes slower (faster) as shown by M. Kato et al. (2025). Their model B (the higher mass accretion rate of $5 \times 10^{-10} M_{\odot} \text{ yr}^{-1}$) shows a much slower rise than that of model A (our original model in the present paper). The earliest ASAS-SN data correspond to the phase after the winds started, and were explained by the free-free emission model light curve (not by the irradiation of the disk). This model B, however, shows much slower rise from $g = 14$ toward the peak as shown in Figure 7 of M. Kato et al. (2025), and is inconsistent with the observation. We safely exclude this model B.

The optical rising timescale of model B is about 2.5 times slower than that of model A. In Figure 8, we plot a 1.5 times longer case (magenta line) than that of model A. Here, we nail down the break in the rising slope of each light curve at HJD 2,459,377.78. The magenta line of free-free emission model V light curve starts from the earliest ASAS-SN data, but the final rise is clearly different from the observation. Therefore, we safely reject the possibility that the ASAS-SN data enter the WD wind phase of the nova. We conclude that the earliest ASAS-SN g data fall in the X-ray flash phase.

5.4. Outburst day

We adopt the outburst day of $t = 0 = t_{\text{OB}} = \text{HJD } 2,459,377.68$ after M. Kato et al. (2025). If we could shift the outburst day slightly later to $t_{\text{OB}} = \text{HJD } 2,459,377.69$, the earliest three ASAS-SN data were observed just on this outburst day (Figure 5(a)). In this case, a brightening-up of ASAS-SN data from $g = 17$ to 16.2 mag could occur within 0.0012 day (= 105 sec).

Then, the timescale of the light curve is 0.9 times compressed compared with our original model. We plot such a model (green line) in Figure 8. The difference between the black line and the green line should be detected because of plenty of observational data near $g = 8-7$. Thus, we safely exclude the case of $t = 0 = t_{\text{OB}} = \text{HJD } 2,459,377.69$ as the outburst day.

6. CONCLUSIONS

Our results are summarized as follows:

1. We present a light curve model for the earliest phase of the V1674 Her outburst, based on the binary model consisting of a $1.35 M_{\odot}$ WD, an irradiated accretion disk and companion star. For the nova explosion model, we used the fully self-consistent nova outburst model of a $1.35 M_{\odot}$ WD with a mass accretion rate of $1 \times 10^{-11} M_{\odot} \text{ yr}^{-1}$ (M. Kato et al. 2025).
2. The first detected optical data (ASAS-SN $g = 17.0$) correspond to $t = 0.34$ hr (0.0144 day) after the onset of thermonuclear runaway, which fall in the X-ray flash phase. The brightness of $g = 17$ mag is consistent with that of an irradiated accretion disk. This ASAS-SN g data clearly shows the X-ray flash phase of a classical nova first detected with an optical band.
3. The g brightness increases/jumps up from the pre-outburst brightness of $g = 19.2$ to $g = 17.0$ mag in the X-ray flash phase. This $\Delta g \sim 2.2$ mag increase is owing to the irradiation effects of the accretion disk. A similar 2.2 mag jumping-up/increase by irradiation effects was first pointed out in millinova outbursts by I. Hachisu & M. Kato (2025). V1674 Her adds another example to this law that hydrogen ignition on a WD makes more than 2.2 mag increase in the disk optical brightness.
4. Optically thick winds emerge from the WD photosphere at $t = 0.96$ hr (0.04 day) after the outburst. As the wind mass-loss rate increases, the dominant source of optical emission changes, after $t = 1.1$ hr (=0.046 day), from photospheric emission of the WD, disk, and companion star to free-free emission of optically-thin plasma just outside the WD photosphere. Our free-free emission model V light curve reproduces the Evryscope g light curve from $g = 14.8$ (at 0.0784 day) to $g = 7.1$ (at 0.2791 day) including a break of light curve slope at $g = 14.3$ (on 0.1 day), where we assume $V - g = 0$.
5. The break in the slope of our free-free emission model light curve is caused by a large increase in the acceleration force due to the strong Fe peak of OPAL opacity. This is the first manifestation of the Fe peak of opacity in the classical nova light curves.
6. There is no indication of strong shocking power in the optical rise between $g = 14.8$ and $g = 7.1$.

Facilities: Swift(XRT), AAVSO

We acknowledge with thanks the variable star observations (V1674 Her) from the AAVSO International Database contributed by observers worldwide and used in this research. We are also grateful to the anonymous referee for useful comments that improved the manuscript.

REFERENCES

- Bhargava, Y., Dewangan, G. C., Anupama, G., C., et al. 2024, MNRAS, 528, 28, <https://doi.org/10.1093/mnras/stad3870>
- Drake, J. J., Ness, J.-U., Page, K. L., et al. 2021, ApJL, 922, L42, <https://doi.org/10.3847/2041-8213/ac34fd>
- Evans, P. A., Beardmore, A. P., Page, K. L., et al. 2009, MNRAS, 397, 1177, <https://doi.org/10.1111/j.1365-2966.2009.14913.x>
- Friedjung, M. 1966, MNRAS, 132, 317, <https://doi.org/10.1093/mnras/132.2.317>
- Habtie, G. R. Das, R., Pandey, R., Ashok, N.M., & Dubovsky, P.A. 2024, MNRAS, 527, 1405, <https://doi.org/10.1093/mnras/stad3295>
- Hachisu, I., & Kato, M. 2001, ApJ, 558, 323, <https://doi.org/10.1086/321601>
- Hachisu, I., & Kato, M. 2006, ApJS, 167, 59, <https://doi.org/10.1086/508063>
- Hachisu, I., & Kato, M. 2022, ApJ, 939, 1, <https://doi.org/10.3847/1538-4357/ac9475>
- Hachisu, I., & Kato, M. 2025, ApJ, 983, 145, <https://doi.org/10.3847/1538-4357/adc107>
- Hachisu, I., Kato, M., & Walter, F. M. 2025, ApJ, 980, 142, <https://doi.org/10.3847/1538-4357/adae08>
- Hachisu, I., Saio, H., Kato, M., Henze, M., & Shafter, A. W. 2020, ApJ, 902, 91, <https://doi.org/10.3847/1538-4357/abb5fa>
- Iglesias, C. A., & Rogers, F. J. 1996, ApJ, 464, 943, <https://doi.org/10.1086/177381>
- Kato, M., & Hachisu, I., 1994, ApJ, 437, 802, <https://doi.org/10.1086/175041>
- Kato, M., Hachisu, I., & Saio, H. 2025, ApJ, in press (arXiv:2506.04615) <https://doi.org/10.48550/arXiv.2506.04615>
- Kato, M., Saio, H., & Hachisu, I. 2022a, PASJ, 74, 1005, <https://doi.org/10.1093/pasj/psac051>
- Kato, M., Saio, H., & Hachisu, I. 2022b, ApJL, 935, L15, <https://doi.org/10.3847/2041-8213/ac85cl>
- Kato, M., Saio, H., & Hachisu, I. 2022c, Research notes of the AAS, 6, 258, <https://doi.org/10.3847/2515-5172/aca8af>
- König, O., Wilms, J., Arcodia, R., et al. 2022, Nature, 605, 248, <https://doi.org/10.1038/s41586-022-04635-y>
- Lin, L, C.-C., Fan, J.-L., Hu, C.-P., Tanaka, J., & Li, K.-L. 2022, MNRAS, 517, L97, <https://doi.org/10.1093/mnrasl/slac117>
- Mróz, P., Król, K., Szegedi, K., et al. 2024, ApJL, 977, L37, <https://doi.org/10.3847/2041-8213/ad969b>
- Muraoka, K., Kojiguchi, N., Ito, J., et al. 2024, PASJ, 76, 293, <https://doi.org/10.1093/pasj/psae010>
- Orio, M., Gendreau, K., Giese, M., et al. 2022, ApJ, 932, 45, <https://doi.org/10.103847/1538-4357/ac63be>
- Patterson, J., Enenstein, J, de Miguel, E., et al. 2022, ApJL, 940, L56, <https://doi.org/10.3847/2041-8213/ac9ebe>
- Quimby, R. M., Metzger, B. D., Shen, K.J., et al. 2024, ApJ, 977, 17, <https://doi.org/10.3847/1538-4357/ad887f>
- Sokolovsky, K. V., Johnson, T.J., Buson, S., et al. 2023, MNRAS, 521, 5453, <https://doi.org/10.1093/mnras/stad887>
- Woodward, C. E., Banerjee D. P.K., Geballe, T.R. et al. 2021, ApJL, 922, L10, <https://doi.org/10.3847/2041-8213/ac3518>